



Tierney, M. J. (2020). Minimum exergy destruction from endoreversible and finite-time thermodynamics machines and their concomitant indirect energy. *Energy*, [117184].
<https://doi.org/10.1016/j.energy.2020.117184>

Peer reviewed version

License (if available):
CC BY-NC-ND

Link to published version (if available):
[10.1016/j.energy.2020.117184](https://doi.org/10.1016/j.energy.2020.117184)

[Link to publication record in Explore Bristol Research](#)
PDF-document

This is the author accepted manuscript (AAM). The final published version (version of record) is available online via Elsevier at <https://doi.org/10.1016/j.energy.2020.117184>. Please refer to any applicable terms of use of the publisher.

University of Bristol - Explore Bristol Research

General rights

This document is made available in accordance with publisher policies. Please cite only the published version using the reference above. Full terms of use are available:
<http://www.bristol.ac.uk/red/research-policy/pure/user-guides/ebr-terms/>

Minimum exergy destruction from endoreversible and finite-time thermodynamics machines and their concomitant indirect energy

Michael Tierney^a

^a*Department of Mechanical Engineering, University of Bristol, Bristol, UK*

Abstract

A functional model of least exergy production (MLED) merges concepts of internal machine irreversibility, reservoir-to-machine thermal resistance, and reservoir-to-reservoir heat links with that of indirect energy used in the manufacture, operation and decommissioning of the engine. Thereupon an analytical solution yields the internal temperatures for the minimum destruction of exergy per unit work. In the absence of heat leaks or internal machine irreversibility, the corresponding cycle efficiency tends to the Carnot efficiency with zero indirect energy, and tends to the [R1:5.4] maximum power efficiency with large indirect energy. A similar approach is applied to a heat pump to yield an optimum coefficient of performance. It is proposed that with adequate databases of cycle irreversibility factors and indirect energy the MLED could be employed as part of a rapid, tentative first step in shortlisting the candidate technologies for localised power and heat supply. In a particular worked example (1) a proposal to replace centrally generated electricity with a local heat engine, fuelled with landfill gas, is rapidly shown to be worthy of a more detailed, structural analysis (2) for both the local and centralised heat engines optimum cycle efficiencies lie between the Carnot efficiency and the maximum power efficiency.

Keywords: Maximum power, Carnot, Indirect energy, Minimum exergy

Nomenclature

MLED model of least exergy destruction

Symbols

		Q	cyclic heat transfer
a, b	coefficients of profit (Eq. 4)	Q_{max}	capacity of machine to receive heat
E_x	cyclic indirect use of energy	r_a, r_b	exergy quality factors
g	cycle fraction	S	entropy
g	cycle time fraction	T	temperature
I_s	cycle irreversibility parameter	W	cyclic work
K	heat transmittance per cycle	x	internal temperature ratio

Greek Symbols

ΔS_{cyc} Cyclic generation of entropy

η cycle efficiency

θ dimensionless temperature

Subscripts

1 hot reservoir

2 cold reservoir

e engine

hp heat pump

i hottest temperature in reversible machine

m optimum

nov Novikov efficiency

ov overall transmittance

rev reversible

Superscripts

' adapts a,b for energy

" adapts a,b for exergy

1 Tentative temperature used to estimate transmittance

1. Introduction

This paper concerns models of least **exergy destruction** (MLED) for idealised engines and heat pumps, allowing for the use of indirect energy. Indirect energy is that energy used to manufacture, operate and decommission a machine. Cycle efficiencies and cycle coefficients of performance are optimised.

When choosing the most sustainable option for locally generating electrical power and heat, the decision maker is faced with the impact of thermodynamic irreversibility - thermal resistance between machines and their surroundings, internal machine irreversibilities and heat leaks between reservoirs. All these lead to irreversible loss of power and concomitant emissions of greenhouse gases. The ecological impact is compounded by the energy demanded indirectly by the manufacture, operation and decommissioning of the engine, and the energy demanded by fuel extraction. Given that manufacturing processes are highly irreversible thermodynamically, the indirect energy employed should be considered in conjunction with a machine's irreversible power loss.

[R1:5.1] The cycle efficiency of an engine is the **useful work produced per unit input of heat**. When an engine operates between two thermal reservoirs the cycle efficiency is [1],

$$\eta = \frac{-W}{Q_1} = 1 - \frac{(-Q_2)}{Q_1} \quad (1)$$

where Q refers to the heat transferred to the engine in one cycle, W refers to the cyclic transfer of work to the engine, subscript 1 refers to the hot reservoir and subscript 2 refers to the cold reservoir. Here the convention is that heat and work flows have positive sign when entering an engine.

Carnot [2] stated that such an engine would offer maximum efficiency if its operation were thermodynamically reversible. A Thermodynamic Temperature scale relates reservoir temperatures uniquely to Q_1 and Q_2 [1] so that,

$$\eta_{rev} = 1 - \frac{T_2}{T_1} \quad (2)$$

[R1:5.2] A simple equation for the efficiency of an endoreversible engine at maximum power is often attributed to Novikov, although Haseli [3] points to Cotterill’s derivation towards the end of the 19th Century [4]. Novikov’s seminal paper [5] concerned atomic power stations and large pools of hot fluids, approximating thermal reservoirs, that transferred heat via a thermal resistance to a thermodynamically reversible engine. Thus a distinction emerged between the hot reservoir temperature T_1 and the engine’s hottest internal temperature T_i . The act of reducing $T_i < T_1$ allowed greater heat transfer into the reversible engine each cycle but at the same time reduced the cycle efficiency. There was thus an optimum $T_{i,m} = \sqrt{T_1 T_2}$, yielding the maximum useful work per cycle. The corresponding cycle efficiency was,

$$\eta_{nov} = 1 - \frac{T_{i,m}}{T_1} = 1 - \sqrt{\frac{T_2}{T_1}} \quad (3)$$

Novikov emphasised the crude nature of his approximation and that it should be treated only as a step preliminary to more detailed calculation. Also, he justified seeking a maximum power output as follows “in contrast to conventional power stations the contribution of fuel costs to the cost of power produced in atomic stations is much less than other contributions, of which the greatest arises from the high capital cost.”

Subsequently Curzon and Ahlborn [6] took the thermal resistances from hot reservoir to engine *and* from engine to cold reservoir and confirmed the maximum efficiency in Equation 3. They claimed a broad agreement with power plant efficiencies in their own present day [6]. This apparent agreement might well have been fortuitous [7][8] because in real-world power stations the transfer of heat from combustion product gases occurs over a range of temperatures and such gases do not constitute a thermal reservoir.

Since Curzon and Ahlborn’s article [6], accommodating the effects of time and heat transfer resistance is often classed as “endoreversible” thermodynamics [9] , **provided that the internal engine cycle operates reversibly. Otherwise the description “finite time thermodynamics” is more appropriate.**

When $T_i > T_1$ the machine operates as a heat pump rather than as a heat engine and the directions of energy flow are reversed. Rather than work and cycle efficiency the indicators are the heat output per cycle and coefficient of performance (COP). Blanchard [10] points out that there is “no natural maximum” for COP with respect to T_i . To constrain the problem of finding the minimum input power for given output heat power Blanchard specified and fixed a variable that combined both the reservoir temperatures and the driving temperature differences. The algebraic solution concludes with optimum COP dependent on machine cold and hot temperatures, reservoir hot temperature and the two reservoir-to-machine resistances.

Alternatively, Sun et al [11] specified the COP to find conditions for an optimum rate of heating. Like Curzon and Ahlborn, their analysis considers thermal resistances at both hot and cold reservoir.

Within non-linear studies heat transfer is not directly proportional to the driving temperature difference. Hoffman and Muschik [12] compare and contrast (1) Novikov versus Carnot engines (2) engines with and without heat leaks (3) “Newtonian” versus “Fourier” conduction. Their “Fourier” mode follows Onsager equations [13] where non-steady processes are driven by differences in reciprocal properties; this is at odds with classical views of “Newtonian” heat transfer where temperature difference acts as the driving force [14]. In Sun et als’ [11] analysis of heat pumps the driving force concerns differences in T^n where n is an exponent.

[R2:2] Several workers have sought an intermediate optimum between the conditions for maximum power and least production of entropy (frequently the Carnot efficiency). De Vos’s [15] [16] thermoeconomic approach optimised the ratio of net work to cost, W/C , termed “profit”. He claimed a different approach to a cost function that considers fuel only [17], or complicated cost functions employing Lagrangian multipliers [18]. De Vos described cost as,

$$C = aQ_{max} + bQ_1 \quad (4)$$

where Q_{max} is a measure of the capacity of the plant and Q_1 is the heat accepted per cycle. Thus aQ_{max} broadly indicates capital costs and bQ_1 broadly indicates fuel costs. In the solution for best W/C there appears a single dimensionless parameter, $\beta = b/a$, upon which it is convenient to present optimum efficiency in terms of “fraction fuel cost”, f (that is the fuel cost as a fraction of total cost of operating a cycle). Thus $f = 0$ leads to the limit of maximum power whereas $f = 1$ leads to the Carnot efficiency.

[R2:2] Many workers have sought the efficiency for a minimum in the ecological function. A first step has been Salamon’s [19] minimisation of the total production of entropy (or the ‘loss of availability’). In considering the impact of finite thermal resistances on several types of engine cycles the maximum cycle work is bounded by,

$$|W| \leq |W_{rev}| - T_o \Delta S_{cyc} \quad (5)$$

where T_o is the temperature of the environment and ΔS_{cyc} is the total cyclic production of entropy. Angulo-Brown [20] subsequently proposed optimising an “ecological function”, as a compromise between the production of maximum power and that of minimum entropy [21]. It has been described as the “power output minus the loss power, which is equal to the product of the environmental temperature and the entropy production rate” [22][23]. A possible criticism is that the two components are arbitrarily weighted equally and one notes Salamon and Nitzan’s [19] earlier “profit function” that in effect weights the component according to their price. The subsequent modified ecological function by Barranco-Jiminez and Angulo-Brown [24] employed a function $\epsilon(\theta_2)$

$$E = |W| - \epsilon(\theta_2)T_o \Delta S_{cyc} \quad (6)$$

where $\theta_2 = T_2/T_1$ and the original unmodified ecological function follows $\epsilon(\theta_2) = 1$. In reference [24] $\epsilon(\theta_2)$ is chosen so as to minimise a second objective function; a ratio of work at maximum power to work at minimum entropy production minus the ratio of corresponding entropies. Yan [25] described this second objective function as “tautological” but nonetheless proceeded to show that $\epsilon(\theta_2)$ depends on the mode of heat transfer; for linear heat transfer $\epsilon_2 = \theta_2^{-0.5}$. Notwithstanding the rebuttal in reference [26] Yan’s form is widely accepted in the subsequent literature. For instance Barranco-Jimenez and Angulo-Brown [24] contrast different heat transfer laws and approaches (e.g. modified ecological versus thermoeconomic). The modified ecological condition results in loss power 50 to 57 % less than that for maximum power.

[R2:2] With regards to heat pumps there has been more emphasis on refrigeration than space heating. Refrigerators are less likely to operate near steady-state, and in addition to the product load they demand analysis of the heat ingress from wall gain and air changes [27]. In addition, Velasco [28] allowed for an irreversibility factor. Maximum cycle COP corresponded to zero cooling power and they proposed instead a per time COP as well as referring to Bejan’s cooling power per unit of capital invested [29]. Their optimisation procedures required time-consuming numerical analysis.

Endoreversible analysis and finite time thermodynamics (FFT) offer potential insight for proposed district heating and total energy schemes, concerning a collection of heat pumps, heat engines, and dissipative processes that **destroy exergy**; examples of the latter include heat losses, heat stores and district heating networks. Whenever power production and district heating are considered for local rather than centralised implementation, a multiplicity of possibly energy schemes might well be considered across a multiplicity of locales. This motivates methods of analysis that swiftly eliminate unsuitable options, as first steps that direct the focus of more time-consuming feasibility studies. Exergetic aspects could well feature in such a study. At this level of very fast analysis calculations should be easily understood and checked with charts and a desk calculator, and the amount of data required should be kept to a minimum. Therefore, we aim to propose a rapid, easily used functional assessment of the reasonableness of the following propositions:

- that a locally cited heat engine might exploit a thermal reservoir to advantage, **destroying less net exergy** than would be the case for centrally generated electricity;
- that the cycle efficiencies of the present-day engines used for a particular class of problem might be further improved;
- that an engine might be used more advantageously as a part of a combined heat and power scheme.

The “functional” models developed in the present paper describe heat engines and heat pumps by their tendency to **destroy exergy**, rather than the physical behaviour of specific “structural” components such as piston-cylinders and heat exchangers.

[R2:4] The objective of the present paper has been to develop analytical expressions that minimise all exergy destruction associated with the generation or use of power, including exergy that is destroyed indirectly. Indirect destruction will occur in the manufacture of a heat engine or heat engine, its operation, its decommissioning, or the extraction of fuel. The scope of the present paper is as follows. A functional model of a heat engine estimates the destruction of exergy by three effects [30]: internal irreversibility, heat leaks, and the thermal resistances between reservoirs and the engine. An important additional term is the indirect exergy, assumed to be converted irreversibly to heat and then dissipated at a standard state temperature, T_o . [R1:1, R2:4] The objective function is thus the total destruction of exergy (indirect plus direct) per unit of exergetic output, as either work or a heating effect. Like the other factors outside the heat cycle - heat leaks and machine costs - the indirect exergy destruction creates a natural optimum without requirement for ecological functions. A worked example is presented, with the objective of studying its emergent properties. These include: (1) very different amounts of indirect energy are attributable to different plant; (2) a local schemes exploiting waste gas is, tentatively, promising when compared with centralised schemes.

2. The Heat Engine

This section concerns modified versions of the Curzon-Ahlborn engine [6], shown in Figure 1. The effects suggested by Chen [30] are implemented, in addition to which indirect energy is explained and accounted for. With regard to the reservoirs of working fluid,

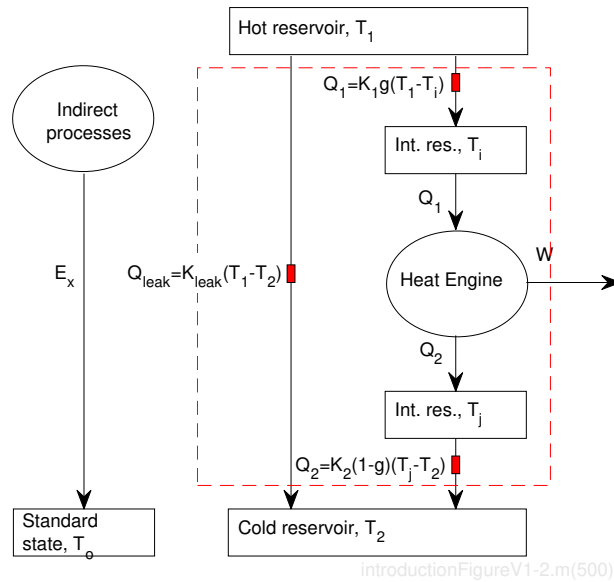


Figure 1: Representation of energy flows for a heat engine. Intermediate reservoirs are at temperatures T_i and T_j , and corresponding heat flows are Q_1 and Q_2 . There is a heat loss Q_{leak} between reservoirs. Independent energy E_x per cycle is attributed to manufacture, operation and decommissioning of the engine and extraction of fuel. Shaded rectangles represent thermal resistances.

the finite thermal transmittance between the hot reservoir (at temperature T_1) and the working fluid restricts the hottest fluid temperature to $T_i \leq T_1$. Similarly the coldest working fluid temperature is restricted to $T_j \geq T_2$. **The essential proposition in this paper is that the energy balance** is augmented by parallel activities contributing an *indirect* energy input per cycle, E_x . This accounts for the manufacture, operation and decommissioning of the engine and possibly takes the form of electrical energy or steam. The operations are assumed to dissipate energy as unrecoverable low-grade heat.

One notes that net inputs of energy/ exergy come from reservoir 1, indirect energy, and net work input. There is a leak of heat from reservoir 1 to reservoir 2. [R1:3] All indirect energy, E_x , is assumed to be converted to heat and dissipated in a reservoir at the standard state temperature, $T_o = 298K$.

2.1. Supporting Thermodynamics

[R2:2],[2.3] Internal reversibilities within a cycle are estimated with a cyclic irreversibility parameter I_s [30], [28]

$$Q_2 = -I_s Q_1 \frac{T_j}{T_i} \quad (7)$$

Here $I_s > 1$ for an engine, $I_s < 1$ for a heat pump, and $I_s = 1$ for an endoreversible machine. Any linear heat leak from the hot reservoir to the cold reservoir is,

$$Q_{leak} = K_{leak}(T_1 - T_2) \quad (8)$$

where K represents a heat conductance. The transfers of heat per cycle become

$$Q_1 = gK_1(T_1 - T_i) \quad (9)$$

and

$$Q_2 = (1 - g)K_2(T_2 - T_j) \quad (10)$$

where cycle time has been divided into a fraction g at which heat is added and a fraction $(1-g)$ at which heat is rejected and any time spent on adiabatic branches is neglected.

Equations 9, 10, and 7, were rearranged to yield heat input Q_1 in a form excluding g [30],

$$Q_1 = \frac{1}{\frac{1}{K_1(T_1 - T_i)} - \frac{I_s T_j / T_i}{K_2(T_2 - T_j)}} \quad (11)$$

Following the First Law of Thermodynamics the cycle work is,

$$W = -Q_1 - Q_2 = -Q_1(1 + I_s \frac{T_j}{T_i}) \quad (12)$$

Chen [30] combined Equations 12 and 11 to give cycle work . He optimised cycle work with respect to internal temperature ratio, $x = T_i/T_j$, and internal temperature T_i to get cycle efficiency at maximum cycle work. It is useful to report cycle efficiency in terms of Equation 1, excluding terms for indirect energy.

2.2. Minimal input of total energy

[R1:2, R2:2] Here we consider briefly the minimisation of all forms of energy used to derive one unit of work. This approach has its limitations, because the energy inputs originate from sources with different exergetic quality factors or chemical exergy factors. For example, whereas the quality factor for electrical supplies is 1.0[31], and the chemical exergy factor for methane is 1.098 [32] [33], the quality factor for heat supplied from a reservoir at twice ambient temperature is only 0.5. Thus sources of geothermal heat and waste heat at comparatively low temperatures hold less value than electricity, fuel, or fluids supplied at comparatively high temperatures. Nonetheless, it is useful to point out that such an approach replicates the economic approach of De Vos [15] .

De Vos [15] optimised W/C where Equation 4 gives cost, C . A potential criticism is that prices fluctuate over the plant lifetime owing to economic influences such as currency exchange rates, learning curves, prices of materials of fabrication, improvements in technology, increasing market penetration of lower cost firms, plus political influences such as tariffs and subsidies. To keep the problem in terms of more consistent thermodynamic and energetic variables Equation 4 is recast in terms of indirect energy, E_x , for this subsection (and in part 2.3.1 as its exergy equivalent),

$$E_x = a'Q_{max} + b'|Q_1| \quad (13)$$

Various estimates of indirect energy are reported openly and also can be derived using proprietary databases such as EcoInvent [34] and freely available databases such as GEMIS [35]. (Further discussion of the derivation of this term is deferred to Section 2.3.1 where it is further recast in terms of exergy.) If discussion is restricted to heat engines with no heat leak then the total energy input is,

$$E_{in} = Q_1 + E_x = a'Q_{max} + (b' + 1)Q_1 \quad (14)$$

This takes practically the same form as the DeVos expression for cost and one optimises W/E_{in} rather than W/C . In comparison with Equation 4, $a' = a$ and $b' + 1 = b$. De Vos treated an endoreversible engine with only a single finite thermal conductance. In terms of the previous subsection $K_2 \rightarrow \infty$, $T_j \rightarrow T_2$, $I_s = 1$.

His condition of lowest cost was in terms of $\theta_2 = T_2/T_1$ and $\beta = b/a$ (or $\beta = (b' + 1)/a$ when energy input replaces cost). The convenient combination of coefficients a and b to a single variable enabled efficiency to be expressed conveniently in terms of the “fuel fractional cost”.

2.3. Minimisation of exergy destruction

The objective function is the exergy destruction per unit of useful exergetic output - work in the instance of a heat engine. In this optimisation, selecting the cold reservoir as the reference state renders exergy destruction practically synonymous with entropy creation, $B_{dest} = T_2\Delta S_{cyc}$. One requires,

$$\frac{\partial(\Delta S_{cyc}/W)}{\partial T_i} \Big|_{T_1, T_2, a'', b'', I_s, x} = \frac{\partial(B_{dest}/W)}{\partial T_i} \Big|_{T_1, T_2, a'', b'', I_s, x} = 0 \quad (15)$$

and

$$\frac{\partial(\Delta S_{cyc}/W)}{\partial x} \Big|_{T_1, T_2, a'_\phi, b'_\phi, I_s, T_i} = \frac{\partial(B_{dest}/W)}{\partial x} \Big|_{T_1, T_2, a'_\phi, b'_\phi, I_s, T_i} = 0 \quad (16)$$

where $x = T_j/T_i$ is the ratio of internal temperatures

Note that B_{dest}/W is related monotonically to $(-W)/(-W + B_{dest})$, a form of exergy efficiency. The choice of T_2 as a reference gives the outlet exergy from the engine proper an apparent value of zero. This exergy was treated not as lost immediately, but as available to other processes such as district heating, and for which any further exergy destruction was reported.

2.3.1. Indirect energy/ exergy addition

[R1:1, R2:1] Equation 13, describing indirect energy, was adapted further.

$$B_x = B_{x, fixed} + B_{x, var} = a''Q_{max} + b''Q_1 \quad (17)$$

The coefficients related to energy were adjusted to account for (1) a change in reference temperature from T_o to T_2 (2) quality and chemical exergy factors

$$a'' = r_a a' \frac{T_2}{T_o}$$

$$b'' = r_b b' \frac{T_2}{T_o}$$

The indirect energy in Equation 13 follows from life cycle analysis, nominally accounting for a sequence of energy contributions that start with the extraction of earth’s resources. The average quality factors r_a and r_b convert a reported energy to its exergy equivalent. All estimates of indirect exergy were assumed to employ the standard state as a reference temperature, $T_o = 298K$. [R1:3] It was also assumed that the complete sequence of indirect processes - manufacturing etc - serves to convert all indirect exergy to heat,

dissipated at T_o . To maintain a consistent generation of entropy, B_x/T_o , the correction T_2/T_o shifts the reference state to the cold reservoir temperature, T_2 .

De Vos's [15] concept of Q_{max} was adapted for a model with two finite conductances (rather than a single finite conductance). Identical intermediate temperatures, $T_i = T_j$, and identical heat flows, $Q_1 = -Q_2$ in Equations 9 and 10, gave,

$$Q_{max} = \frac{T_1 - T_2}{1/(g_m K_1) + 1/((1 - g_m) K_2)} = K_{ov}(T_1 - T_2) \quad (18)$$

Where K_{ov} describes an overall conductance. The value of fraction g that in turn optimised Q_{max} was,

$$g_m = \frac{1}{1 + \sqrt{K_1/K_2}} \quad (19)$$

2.3.2. Exergy balance

Given the reference temperature T_2 the net cyclic exergy inputs were,

$$\begin{aligned} B_1 &= Q_1 \times \left(1 - \frac{T_2}{T_1}\right) = Q_1(1 - \theta_2) \\ B_2 &\equiv B_{leak} = Q_{leak} \times \left(1 - \frac{T_2}{T_1}\right) = K_{leak} T_1 (1 - \theta_2)^2 \\ B_3 &\equiv B_x = a'' Q_{max} + b'' Q_1 \\ B_4 &\equiv W = -Q_1 - Q_2 = -Q_1(1 - I_s x) \end{aligned}$$

where Q_1 , Q_{leak} , B_x , and W follow respectively from Equations 11 8, 17, and 1. The above were summed to give exergy destruction, yielding the exergy destruction per unit work,

$$\frac{B_{dest}}{|W|} = \frac{\sum B_i}{-W} = \frac{B_{leak} + a'' Q_{max}}{+Q_1(1 - I_s x)} + \frac{+Q_1((1 - \theta_2) + b'' - (1 - I_s x))}{+Q_1(1 - I_s x)}$$

Substitution of the heat flow Q_1 from Equation 11 yielded,

$$\frac{B_{dest}}{|W|} = \frac{\sum B_i}{|W|} = \left| \frac{c_1}{1 - I_s x} \times \left(\frac{1}{1 - \theta_i} - \frac{c_2 x}{\theta_2 - x \theta_i} \right) + \frac{c_3 + I_s x}{1 - I_s x} \right| \quad (20)$$

where for algebraic convenience,

$$\begin{aligned}\theta &\equiv T/T_1 \\ x &\equiv T_j/T_i \\ c_1 &\equiv \frac{B_{leak} + a''Q_{max}}{K_1T_1} \\ c_2 &\equiv K_1I_s/K_2 \\ c_3 &\equiv b'_\phi - \theta_2\end{aligned}$$

Figure 2 plots scaled exergy destruction against the scaled intermediate temperature, $\theta_i = T_i/T_1$, and for a particular scaled cold reservoir temperature $\theta_2 = T_2/T_1 = 0.5$. The calculation is completed for a range of a'' and for $b'' \in \{0, 0.25\}$, an endoreversible engine ($I_s = 1$) and single finite conductance ($K_2 \rightarrow \infty$). Each minimum is indicated by an asterisk (*). [R1:4] Increasing θ_i above its optimum value, $\theta_{i,m}$, increased cycle efficiency, but at the cost of less work produced per cycle so that the fixed rates of exergy destruction - indirect and heat leak terms - gained greater relative importance. With no fixed component of indirect energy, $a'' = 0$, there are no minima and the best conditions for an engine are at $\theta_i = 1$. Minima are evident for all other values of a'' . The non-zero component of indirect energy, $b'' = 0.25$, increased exergy destruction and increased the optimum $\theta_{i,m}$ for a heat engine. As $a'' \rightarrow \infty$ then the curves for the two values of b'' appear coincident. The minimum at $\theta_{i,m} = \sqrt{\theta_2}$, coincided with the endoreversible condition for maximum power.

2.4. Optimisation

Equation 20 for B_{dest}/W was differentiated to obtain a minimum value. The first operation was with respect to the scaled intermediate temperature, θ_i so that, and the two roots for $\theta_i = T_i/T_2$ are,

$$\frac{\partial(B_{dest}/|W|)}{\partial\theta_i} = 0 \implies \theta_{i,m} = \frac{\theta_2 + c_x^{1/2}x}{x + c_x^{1/2}}$$
(21)

where $c_x = \pm c_2$ and the appendix demonstrates that only $c_x = c_2$ is legitimate. This optimum was substituted back into Equation 20 before differentiation with respect to x , the ratio of intermediate temperatures, $x = T_j/T_i$.

$$\frac{\partial(B_{dest}/|W|)}{\partial x} = 0 \implies x_m = \frac{I_s\theta_2 \pm \chi}{(I_s + I_sc_1 + I_sc_3 + I_sc_1c_2 + 2I_sc_1c_2^{1/2})}$$
(22)

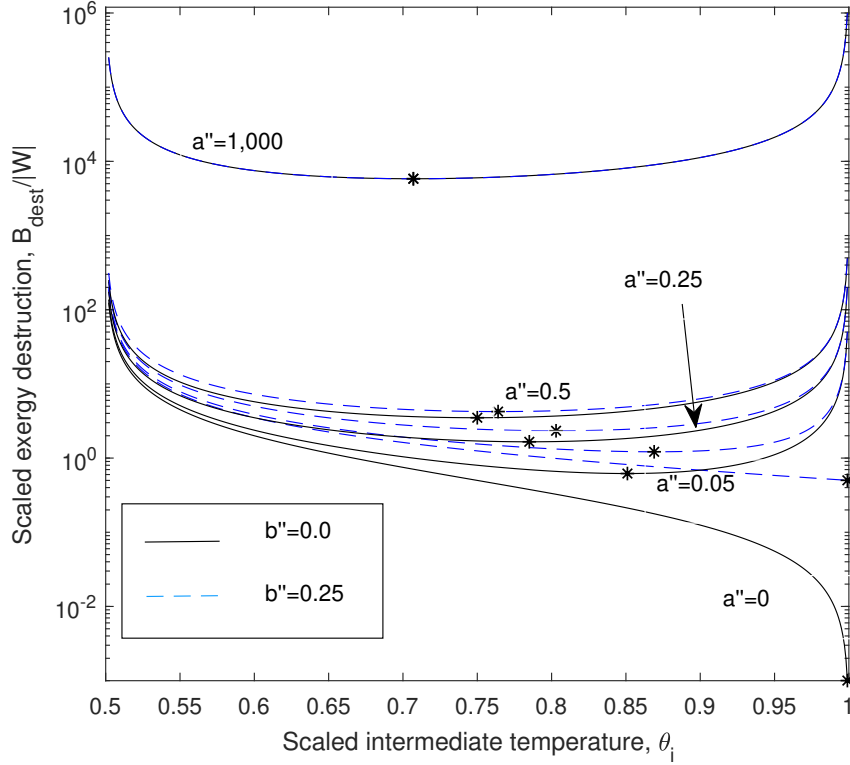


Figure 2: Impact of scaled intermediate temperature, θ_i , on exergy destruction per unit work. The scaled cold reservoir temperature is $\theta_2 = 0.5$. $I_s = 1$. * indicates a minimum value.

where

$$\chi = (I_s c_1 \theta_2 (c_1 + c_3 - I_s \theta_2 + c_1 c_2 + 2c_1 c_2^{1/2} - I_s c_3 \theta_2 + 1))^{1/2} + \dots$$

$$c_2^{1/2} (I_s c_1 \theta_2 (c_1 + c_3 - I_s \theta_2 + c_1 c_2 + 2c_1 c_2^{1/2} - I_s c_3 \theta_2 + 1))^{1/2} + I_s c_3 \theta_2$$

The larger value of the temperature ratio conforms to $x_m \geq \theta_2$ for a heat engine.

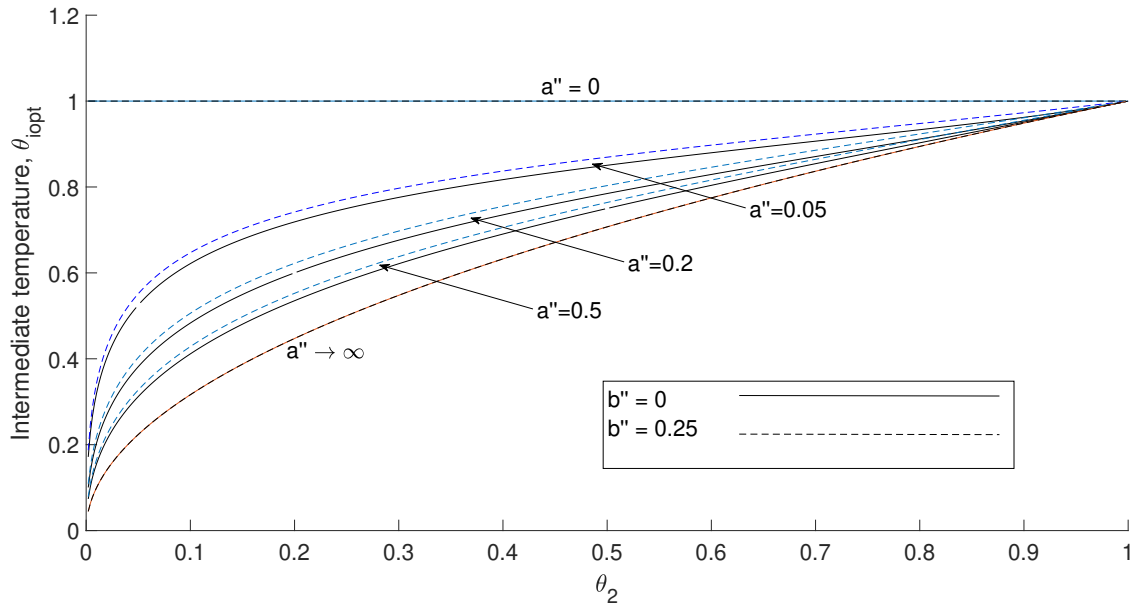
The unwieldiness of Equation 22 in particular could result in coding errors in spreadsheets or computer programmes and symbolic computation is recommended. For the purposes of a simpler equation, one can apply zero resistance to heat rejection, $K_2 \rightarrow \infty$. Thereupon $g = 1$, $T_j \rightarrow T_2$ and $c_2 \rightarrow 0$.

$$\theta_{i,m} = \frac{((I_s \theta_2 c_1 (c_1 + c_3 - I_s \theta_2 - I_s \theta_2 c_3 + 1))^{1/2} + I_s \theta_2 + I_s \theta_2 c_3)}{(I_s \theta_2 - c_1 + I_s \theta_2 c_3)}$$

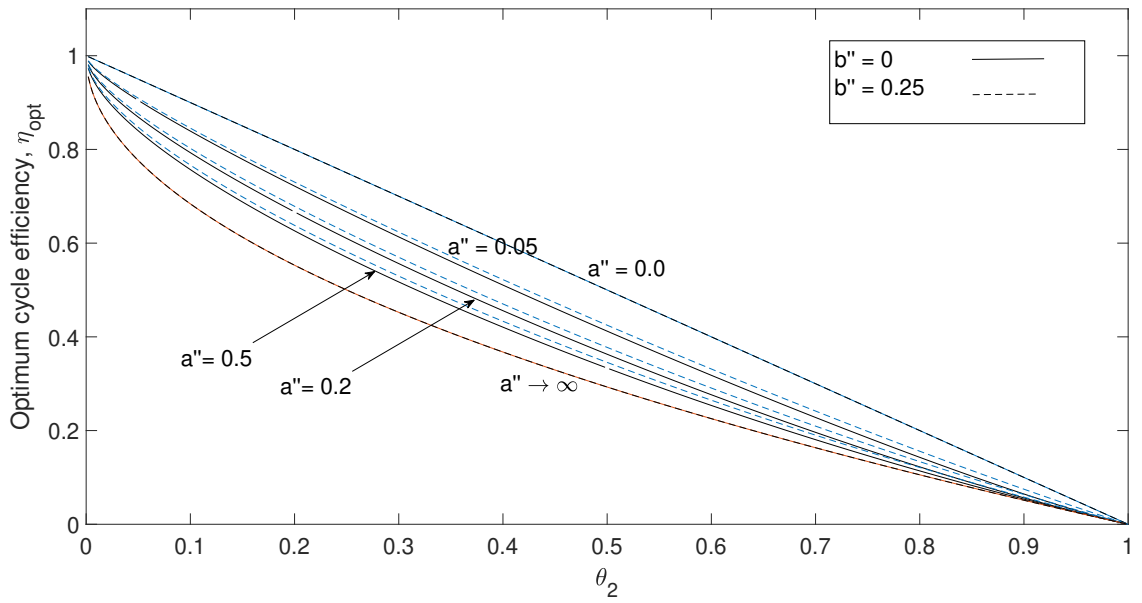
An endoreversible engine with single resistance and no heat leak was simulated ($I_s = 0$ and $K_2 \rightarrow \infty$ at which $c_1 = a'_\phi$). Results shown in Figure 3 confirm expected trends. With no heat leak or internal irreversibility ($Q_{leak} = 0$ and $I_s = 1$): (1) the Carnot limit is reached at zero fixed indirect exergy, $a'' = 0$;

(2) the limit of maximum power is reached at infinite fixed direct energy, $a'' \rightarrow \infty$; (3) at either of these extremes, changing from $b'' = 0$ to $b'' = 0.25$ has minimal effect on the optimum; (4) in the intermediate range, increasing variable indirect energy moves the optimum towards the Carnot solution.

Figure 4 investigates the impact of model parameters on optimum cycle efficiency, $\eta_{opt} = |W|/Q_1$. The baseline duplicates the conditions for Figure 3. In one study the thermal resistances were divided equally, $K_1 = K_2 = 4$ so that in Equation 18 the term Q_{max} held the same value as the default case where $K_1 = 1, K_2 \rightarrow \infty$. The change in efficiency from the baseline, at most 0.4%, is not discernible in part(a). As is also shown in Figure 3, a large coefficient of fixed indirect energy, $a'' = 1000$, forced the solution towards the limit for maximum power. A finite heat leak, $K_{leak} = 0.2$, had the same effect, which is unsurprising because for fixed T_1 and T_2 both heat loss and fixed component of indirect heat are constants. Increasing I_s unsurprisingly reduced the cycle efficiency. On part (b) of Figure 4 individual parameters were varied between a minimum value (Val_{min}) and a maximum value (Val_{max}), represented by a fraction between 0 and 1 on the x-axis. The trends in part (a) reoccur in part (b) across ranges of parameters. Increasing the variable indirect energy use through parameter b'' would ultimately result in the maximum Carnot efficiency whereas increasing the fixed indirect energy use (parameter a'') forced the solution towards the limit of maximum power. On part (b) a horizontal line indicates a range of transmittance K_1 , applied with a commensurate reduction in K_2 to give a constant Q_{max} according to Equation 18. There was no appreciable change in $\eta_{cyc,m}$. Also K_1 was increased, with $K_2 = K_1$, resulting in a change in Q_{max} (indicated by an asterix, *). This also had no effect because the direct addition of heat, Q_1 , and the indirect addition, $a'' \times Q_{max}$, were in approximate proportion to each other.

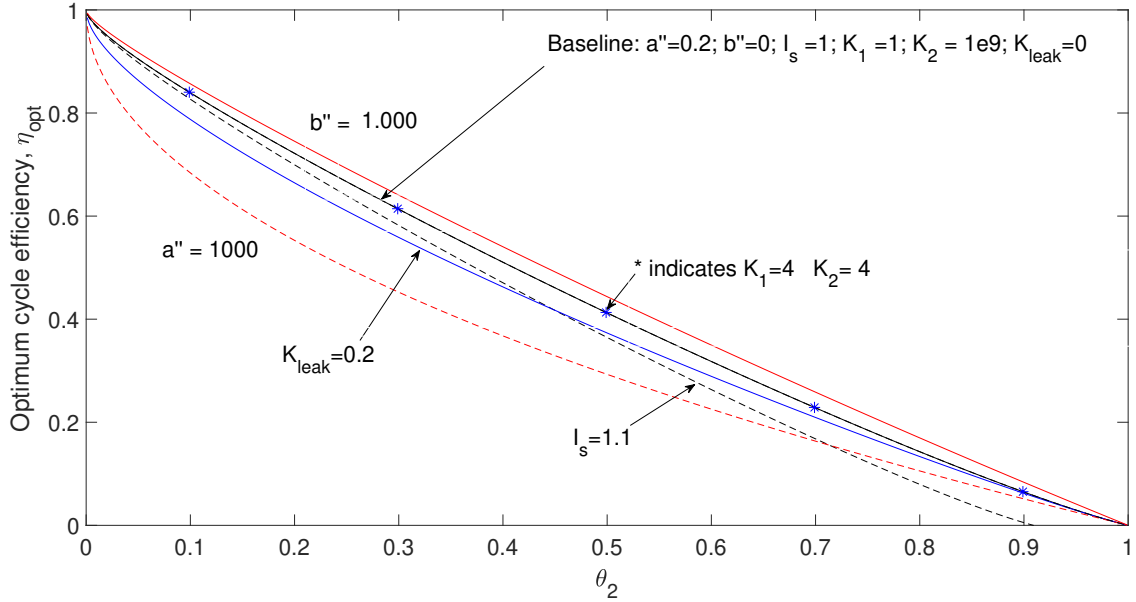


(a)

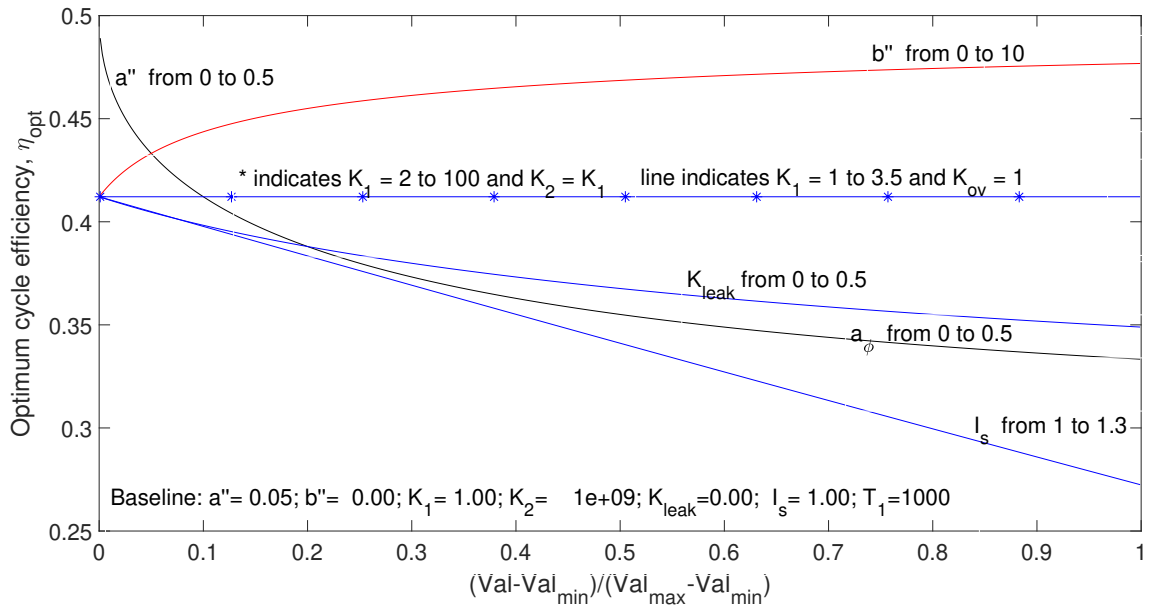


(b)

Figure 3: Heat engine at point of minimum exergy destruction (a) optimum hot temperature (scaled) $\theta_{i,m} = T_{i,m}/T_1$ (b) cycle efficiency, $|W|/Q_1$. $K_2 \rightarrow \infty$, $I_s = 1$



(a)



(b)

Figure 4: Survey of heat engine model (a) Cycle efficiency ($|W|/Q_1$) versus scaled sink temperature (b) Parametric survey, with variations in a'' , b'' , K_{leak} , K_1 , I_s , K_{ov} from minimum to maximum value. The baseline is a single reservoir model with reversible internal engine, no heat leak, and fixed indirect exergy determined by $a'' = 0.2$ (part a) or $a'' = 0.05$ (part b). Also $T_1 = 1000$ and $\theta_2 = 0.5$.

3. The Heat Pump

This section concerns the optimum COP of a heat pump. Rather than the production of mechanical work W , the objective is the transfer of heat, Q_1 , to the hot reservoir. The COP is thus defined as

$$COP = -\frac{Q_1}{W} = \frac{Q_1}{Q_1 + Q_2} \quad (23)$$

The scheme for the heat pump was similar to Figure 1 except that the directions of energy flows Q_1, Q_2, W were reversed.

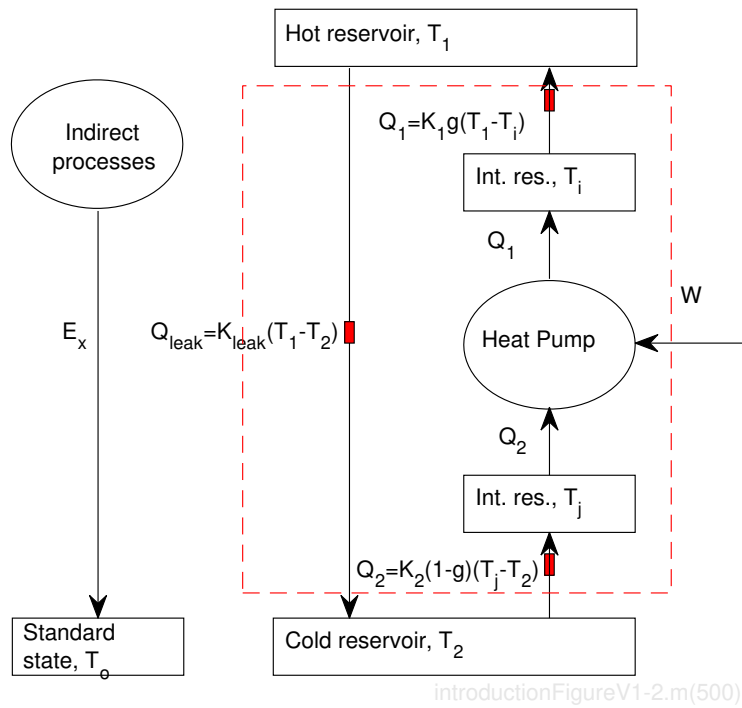


Figure 5: Representation of energy flows for a heat pump, similar to Figure 1 for a heat engine but with reversal of some energy flows. Here $T_i > T_1$ and $T_j < T_2$ (NB: Label “Heat Engine” should be Corrected to “Heat Pump”)

[R1:1] The objective function was the destruction of exergy per unit of useful exergetic output of the plant. The latter was attributed to heating effect,

$$B_{out} = (-1) \times B_1 = -Q_1 \left(1 - \frac{T_2}{T_1}\right) = -Q_1 (1 - \theta_2) \quad (24)$$

Terehovics [36] used a similar form in an analysis of district heating, with T_1 equal to the logarithmic mean of flow and return temperatures and T_2 taking the place of ambient temperature. The objective function is

then,

$$\frac{B_{dest}}{B_{out}} = \frac{\sum B_i}{(-1) \times Q_1(1 - \theta_2)} = \frac{B_{leak} + a'' Q_{max}}{(-1) \times Q_1(1 - \theta_2)} + \frac{(-1) \times Q_1((1 - \theta_2) + b'' - (1 - I_s x))}{(-1) \times Q_1(1 - \theta_2)}$$

The substitution of heat transfer Q_1 from Equation 11 yielded,

$$\frac{B_{dest}}{B_{out}} = \frac{c_1}{1 - \theta_2} \times \left(\frac{1}{1 - \theta_i} - \frac{c_2 x}{\theta_2 - x\theta_i} \right) + \frac{c_3 + I_s x}{1 - \theta_2} \quad (25)$$

where the coefficients c_1, c_2, c_3 were defined after Equation 20. The denominator $(1 - I_s x)$, previously applicable to a heat engine, was replaced with $(1 - \theta_2)$. The optimum temperature ratio was,

$$x_m = \theta_2 \pm \sqrt{\theta_2/I_s}(\sqrt{c_1} + \sqrt{c_2}) \quad (26)$$

and the lower estimate ensured $x_m < \theta_2$ but was unrealistic when $x_m \leq 0$. The optimum intermediate temperature, $\theta_{i,m}$, appeared in the same form as that for the heat engine, Equation 21.

$$\theta_{i,m} = \frac{\theta_2 + c_2^{1/2} x}{x + c_2^{1/2} x}$$

Following the analysis of heat engines, the indirect exergy was related to Q_1 and Q_{max} . The negative sign of Q_1 necessitated a negative value of coefficient b'' . Unlike a heat engine, the product $b'' \times Q_1$ has no relation to the extraction of fuel, but might well be attributed to the parasitic fan or pump power.

Figure 6 replicates an earlier plot for a heat engine by presenting in scaled forms exergy destruction versus intermediate temperature. With no fixed component of indirect energy, $a''_\phi = 0$, the optimum condition lies at $\theta_{i,m} = 1$, indicated by an asterisk (*). Thereupon increasing a'' increased $\theta_{i,m}$ whereas the term b'' increased exergy destruction but had no influence on the optimum condition. The minima were far less distinct than those in Figure 2. In the limit $\theta_i \rightarrow 1$ there was zero exergetic output but a finite demand for indirect exergy and $B_{dest}/B_{out} \rightarrow \infty$. The objective function approached an asymptote as $\theta_i \rightarrow \infty$.

Figure 7 presents the sensitivity of optimum conditions to different levels of indirect exergy, $a'' \times Q_{max}$ and $b'' \times Q_1$. Part (a) shows the scaled intermediate temperature and part (b) shows the corresponding coefficient of performance. Changes in the variable indirect exergy, $b''Q_1$, had no effect on the optimums (this is also apparent in Figure 6). Unrealistic optimums, $\theta_{i,m} < 0$ and not plotted in part (a), existed below critical θ_2 and caused $COP < 1$ in part (b).

Figure 8 further investigates the impact of model parameters. On part (a), applying a variable indirect

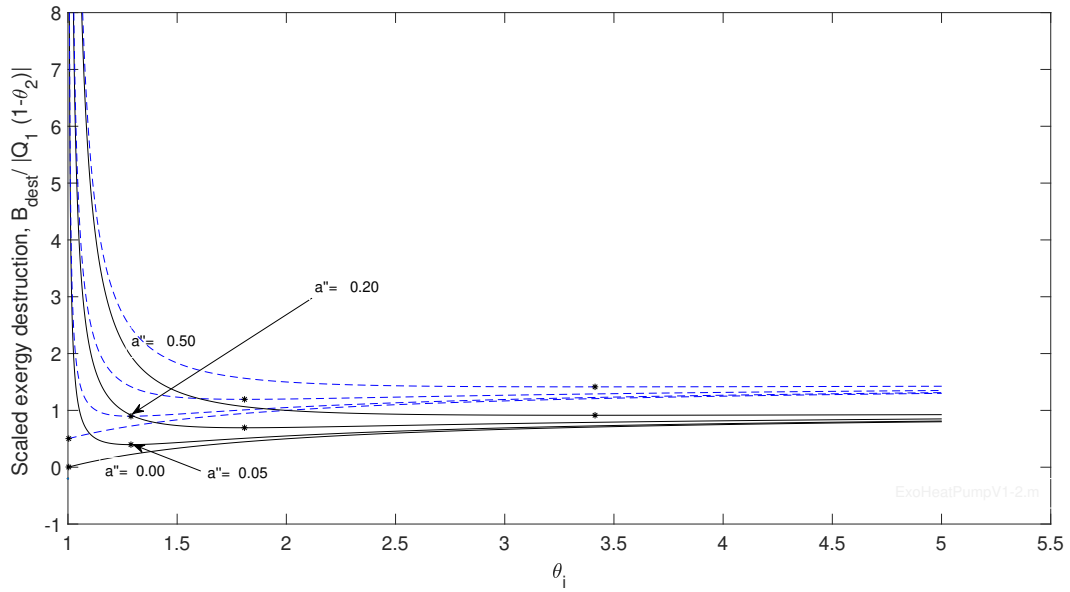
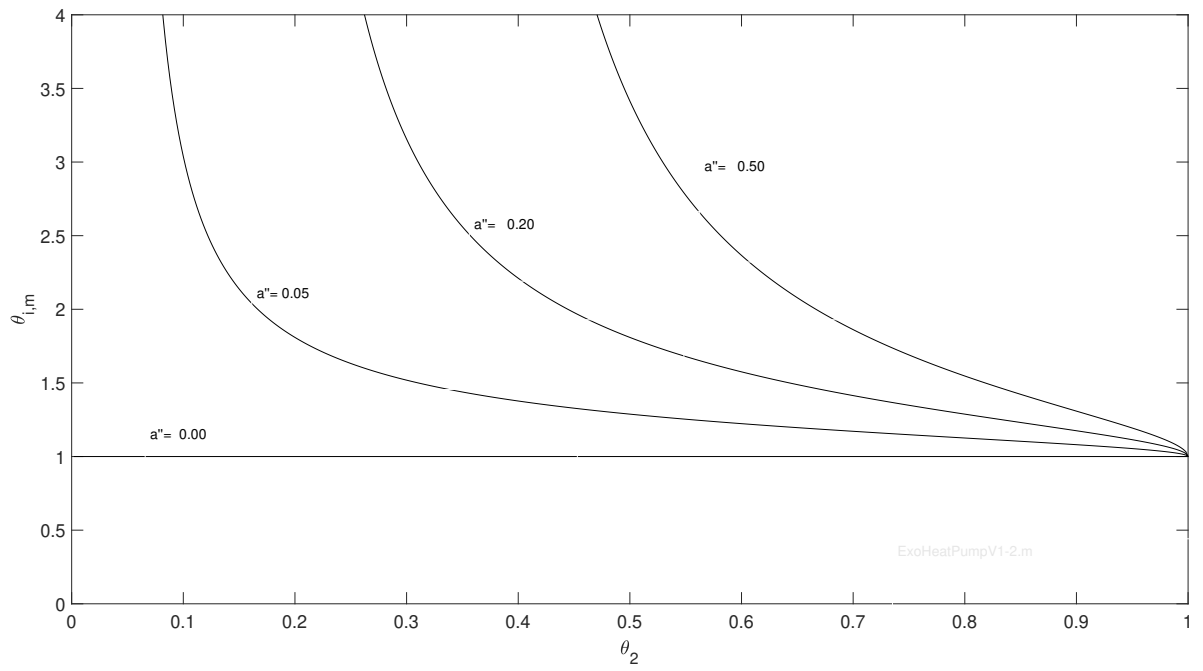
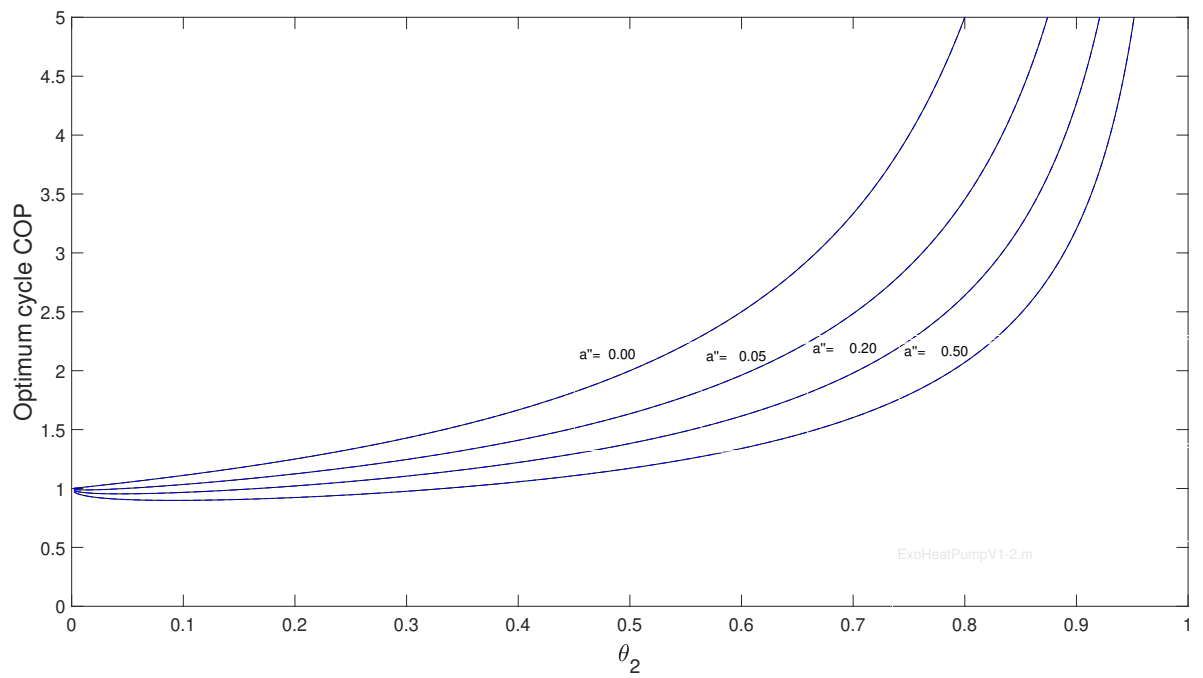


Figure 6: Impact of **scaled** intermediate temperature, θ_i , on exergy destruction per unit work in a heat pump. Here $\theta_2 = 0.5$, $T_1 = 1000$, $K_1 = 1$, $K_2 \rightarrow \infty$, $I_s = 1$,. Values of b_ϕ are 0 (solid lines), -0.25 (dashed lines)

exergy/energy, did not change the optimum cycle COP compared to the baseline (hence the + symbol, used to identify $b'' = -0.25$, lies on the solid curve for default conditions). For the same K_{ov} and Q_{max} , changing from a governing transmittance to two equal transmittances also had no discernable impact (the * symbol indicating $K_1 = K_2 = 4$ also lies on the solid curve for baseline). In both parts(a) and (b) a reduction in a'' gave a higher cycle COP (there is an instance of $a'' = 0$ on part (a) and a'' is varied from 0 to 0.5 in part (b)). A heat leak or reduction in I_s reduced the optimum cycle COP.

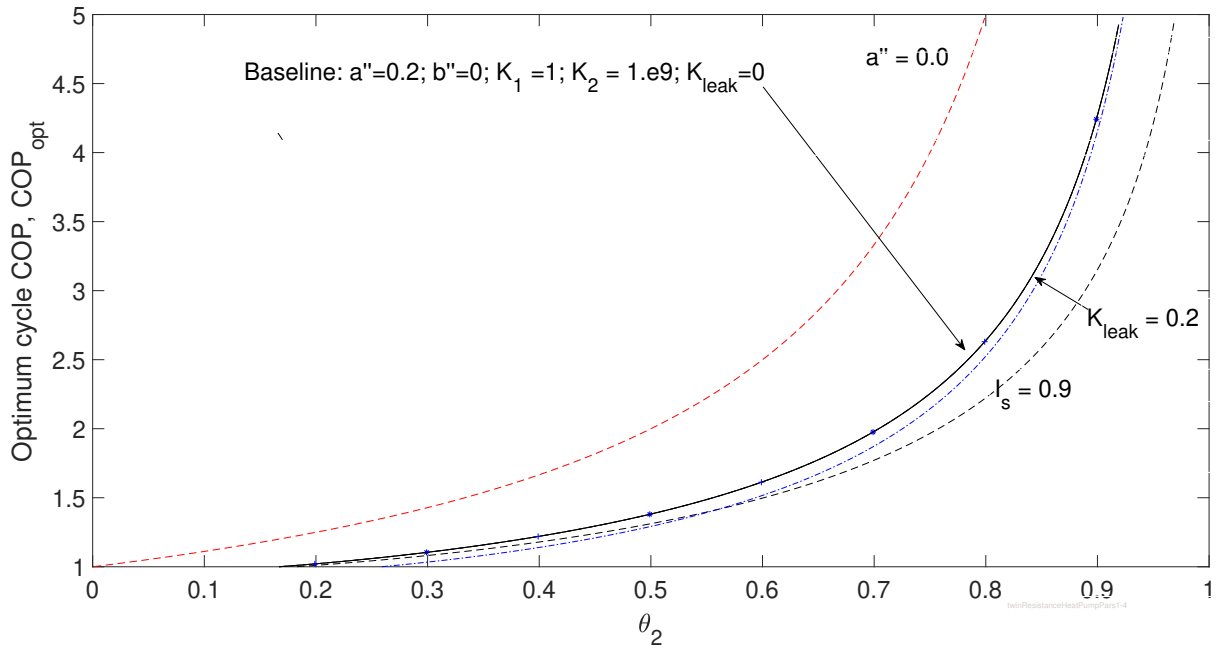


(a)

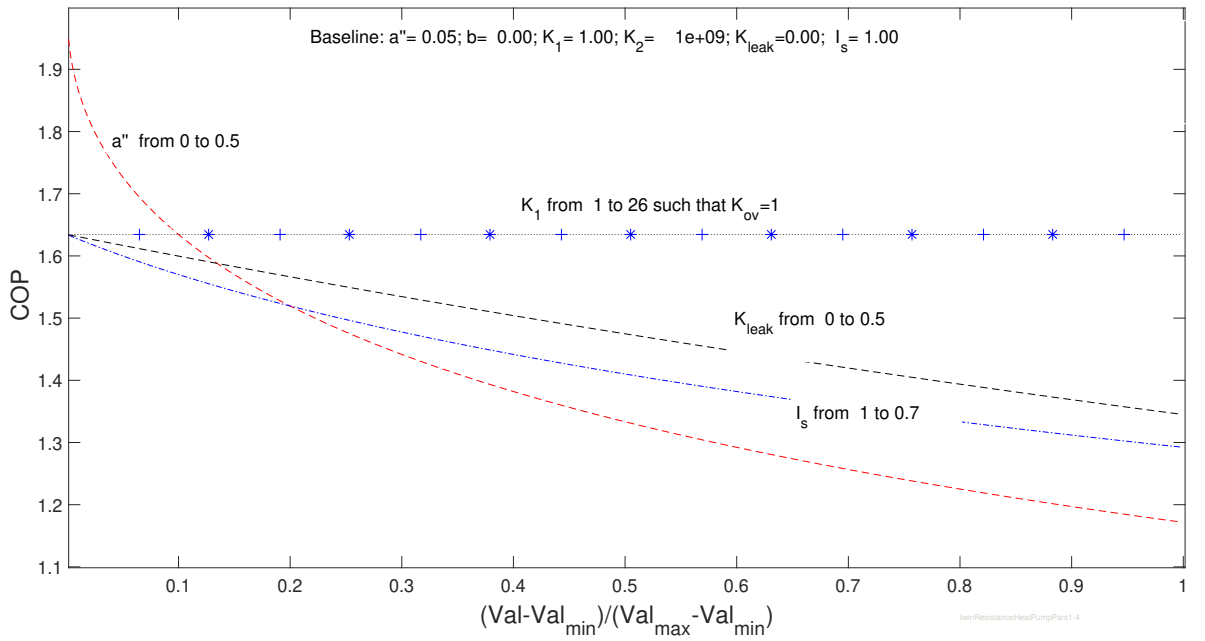


(b)

Figure 7: Heat pump at point of minimum exergy destruction (a) optimum internal temperature (scaled) $\theta_{i,m} = T_{i,m}/T_1$ (b) optimum coefficient of performance, $|W|/Q_1$. Curves for $b'' = 0$ and $b'' = -0.25$ coincide.



(a)



(b)

Figure 8: Survey of heat pump model (a) coefficient of performance ($|Q_1/W|$) versus scaled sink temperature (b) parametric survey, with variations in a'' , b'' , K_{leak} , K_1 , I_s , K_{ov} from minimum to maximum value. The baseline is a single thermal resistance model with reversible internal engine, no heat leak, and fixed indirect energy determined by $a'_\phi = 0.2$ (part (a)) or $a'_\phi = 0.05$ (part (b)). Symbols are: * $K_1 = K_2 = 4$; + indicates $b'_\phi = -0.2$. Also $T_1 = 1000$ and $\theta_2 = 0.5$ in part (b)

4. Cyclic Dissipative Processes

A dissipative process transfers heat between two or more thermal reservoirs with no derivation of useful work. Dissipative processes can undergo diurnal or seasonal cycles. Examples include heat stores, heat transmission networks and heat losses. Let Q_1 here be the heat transfer from a reservoir at temperature T_1 to a reservoir at temperature T_2 . Here no work is concerned, $W = 0$, and there are no intermediate temperatures. The associated exergy input is,

$$B_{heat} = Q_1(1 - \theta_2) \quad (27)$$

A scaled estimate of exergy destruction is,

$$\frac{B_{dest}}{B_{heat}} = 1 + \frac{Q_{leak}}{Q_1} + \frac{rE_x}{Q_1(1 - \theta_2)} \quad (28)$$

Because $W = 0$, $Q_{max} = Q_1$ yielding,

$$\frac{B_{dest}}{B_{heat}} = 1 + \frac{K_{leak}}{K_1} + \frac{a''_{\phi} + b''_{\phi}}{1 - \theta_2}$$

where K_{leak} , K_1 are conductances between reservoirs. There is no internal temperature with respect to which this exergy production can be minimised, and likewise there is no minimum value with respect to θ_2 .

5. Worked Example

[R3:3] The limitations of the models of least exergy destruction (MLED) are explored by means of a worked example so as to elicit its emergent properties. It concerns a source of landfill gas located 800 metres from a village [37]. The original, publicly available, commercial report considered 15 case studies in the South Western United Kingdom, each serving as the first in a sequence of stage-gates, leading potentially to feasibility studies and the design of local sustainable energy sources. The selected study typifies discussions concerning the feasibility of sustainable energy schemes in this region. The original report presents purely discursive analysis that often rejects the possibility of local energy schemes in favour of existing central production of electricity and gas; this has motivated a search for a rapid analytic solution. The two postulated alternatives are: (1) a central power station generates sufficient electricity both to satisfy the stated electricity consumption and to drive heat pumps that meet the heating requirement; (2) a local heat engine fuelled with the landfill gas generates the required electricity - some rejected heat is diverted to a district heating network. Table 1 presents [R3:3] the rated machine sizes in [37] plus the assumed part load uses of heat and power. Table 1 also includes estimates of indirect energy for the various plant items. The indirect energy of the district heating loop was estimated from that of the individual components listed in Table 1, spread over a lifetime of 30 years. The areas and masses of heat exchanger tube were found assuming a overall heat transfer coefficient of $150W/m^2K$. By far the largest contribution was the fabrication of piping from virgin steel. [R3:4] Even if the use of recycled steel had been assumed (rather than virgin steel), producing a three-fold reduction in indirect energy, pipe fabrication would still have formed the largest contribution to indirect energy. The heat loss allowed for pipes (converted to indirect energy by assuming a COP of 4.5) was only $190/42\,236 = 0.4\%$ of indirect energy.

Figure 9 shows on an annual basis two sets of estimated energy flows for the centralised generation of electricity. The values can be worked out from coefficients of performance and engine efficiencies that follow from models of least exergy destruction (MLED) in part (a) and present-day values in part (b). Thermal reservoirs are shown as rectangles and heat engines and heat pumps as circles, annual flows of energy are presented in GJ and annual exergy destruction attributable to machines in GJ. Table 2 summarises the present-day efficiencies used in part (b), and the values of T_i and E_x employed to obtain the theoretical efficiencies used in part (a). In particular the present-day cycle efficiency of a Rankine cycle with superheat and reheat is 40% [45] and the boiler efficiency was taken as 88%. To facilitate comparisons with later estimates, combustion gas temperatures were assumed to range from 1300 K to 400 K and the logarithmic mean was used as the reservoir temperature, $T_1 = 764K$.

The reported ratios E_x/W for coal burning plant and E_x/Q_1 for a heat pump were applied to get the fixed component of indirect exergy.

Table 1: Contributions to energy flows

Item	Comments	Energy per unit mass or volume		Ref.	Energy, MJ/yr
		Range	Mid point		
<u>Annual energy consumption</u>					
Heating (rating 2.5 kW)	49% capacity			[37]	38 242 250
Elec. (rating 2.74 kW)	85% capacity			[37]	73 456 660
<u>Indirect energy - coal station</u>					
Whole plant	$E_x = 0.117W$			[38]	9 276 927
<u>Indirect energy - heat pump</u>					
Whole unit	$E_x = 0.106Q_1$			[39]	4 053 679
<u>Indirect energy - gas turbine</u>					
Construction				[40]	18 550
Maintenance				[40]	534 638
Parts				[40]	349 847
<i>Grand total - indirect energy of turbine</i>					903 035
<u>Indirect energy - district heating spread over 30 years</u>					
<i>Dual pipe EN253 -DN80 schedule [41], , buried in 850 x 900 mm trench [42]</i>					
Fabrication	1600m × 21.4kg/m	33MJ/kg	33MJ/kg	[43]	37 576
<i>Excavate trench, evacuate, off-site disposal</i>					
Excavation	800 m	14 – 89MJ/m ³	52 MJ/m ³	[44]	
Evacuate + Transport		19 – 135MJ/m ³	77MJ/m ³	[44]	
Sub total					2 632
<i>Heat exchangers - exhaust gas to DH loop and DH loop to housing</i>					
Exhaust to DH	844 kg				
DH to housing	512 kg				
All heat exchangers		33MJ/kg	33MJ/kg	[43]	1 492
<i>Operation of district heating</i>					
Pumping	1600 m loop	11W/m	11W/m	[41]	347
Heat losses - elec. equivalent					
Flow (90°C)	COP=4.5	17.7W _{th} /m	3.9W _e /m	[41]	
Return (40°C)	COP=4.5	6.4W _{th} /m	1.4W _e /m		
Total heat loss					190
<i>Grand total - indirect energy of district heating</i>					42 236

Heat engine

$$B_{x, fixed} = a'' Q_{max} = 0.117W_{re}$$

Heat pump

$$B_{x, fixed} = a'' Q_{max} = 0.106Q_{1, re}$$

where re indicates the requirements at the top of Table 1, $Q_{1,re} = 38TJ$ and $W_{1,re} = 73TJ$ approximately. (Treating the quality factor as 1.0 resulted in $E_x \equiv B_x$.) A tentative estimate of the average temperature difference between furnace gases and steam, $T_1 - T_i^1 = 235K$, was employed to estimate transmittance coefficient K_1 . This tentative temperature difference corresponded to: a Rankine cycle with superheat to 150 bar and 823 K, and reheat to 70 bar and 823 K; a condenser temperature of 323 K; weighting of the logarithmic mean temperature differences for feedwater heating, boiling, superheating and reheating according to their heat transfers to obtain a mean temperature difference [1]. In order to estimate the conductance terms K_1, K_2 it was assumed additionally that $g = 0.5$ and that the driving temperature difference across any condenser was $T_2 - T_j^1 = 10K$, and that the 'present day' cycle efficiency was applied to give the heat transfer to the condenser. With rearrangement of Equations 9 and 10,

$$K_1 = \frac{Q_{1,pd}}{g(T_1 - T_i^1)}$$

$$K_2 = \frac{Q_1(1 - \eta_{cyc,pd})}{(1 - g)(T_j - T_2^1)}$$

where "pd" indicates a present day estimate and $Q_{1,pd} = W/\eta_{cyc,pd}$. For the heat pump $g = 0.5$ was retained and driving temperature differences were taken as $T_i^1 - T_1 = 15^\circ C$ [46] and $T_j^1 - T_2 = 14^\circ C$ [47], hence

$$K_1 = \frac{Q_1}{g(T_1 - T_i^1)}$$

$$K_2 = \frac{Q_1(1 - 1/COP_{pd})}{(1 - g)(T_j - T_2^1)}$$

Table 2: Efficiencies for centralised power generation

Heat Engine			Heat Pump		
Item	Value	Notes	Item	Value	Notes
<u>Present day values</u>			<u>Present day values</u>		
Cycle Efficiency	35.2%		COP	3.0	[48]
E_x/W	0.117	[38]	E_x/Q_1	0.106	[39]
T_1	764K		T_1	291K	
T_2	291K		T_2	283K	
<u>Estimates for optimisation</u>			<u>Estimates for optimisation</u>		
Q_{leak}	$0.136 \times Q_1$		Q_{leak}	0	
I_s	1.166		I_s	0.9	
T_i^1	$T_1 - 235K$		T_i^1	$T_1 + 15K$	[46]
T_j^1	$T_2 + 10K$		T_j^1	$T_2 - 14K$	[47]
<u>Efficiencies</u>			<u>COPs</u>		
Present-day	35.2%		Present-day	3.0	[48]
MLED- cycle	46.8%	,	MLED-cycle	4.38	,
MLED-plant	41.1%	,	MLED	4.38	,
Carnot	61.9%		Carnot	36.4	
Maximum power [5]	38.3%				

The analysis from the MLED is presented on Part (a) of Figure 9, as well as Table 2. In the heat engine and heat pump, the reported exergy destructions (indexed with an asterisk, *) followed from,

$$B_{dest} = -T_o \left(\frac{Q_1 + Q_{leak}}{T_1} + \frac{Q_2 - Q_{leak}}{T_2} \right)$$

where $T_o = 298K$. The indirect term is shown separately on the Figure, with an assumed quality factor of unity so that $E_x \equiv B_x$. Under optimum operation, annual heat inputs comprised 175 513GJ direct to the engine, 23 870GJ as a heat leak between reservoirs, and 13 671GJ of indirect energy; the resulting total exergy destruction by the machines was 42 675GJ in addition to the indirect contribution. In Table 2, The engine cycle efficiency of 46.8% (by MLED) was closer to the maximum power efficiency than the Carnot efficiency.

[R1:4] At this point Table 3 reports the sensitivities of performance indicators to heat leaks, indirect energy, I_s , and thermal transmittance, K_1 . The trends are as expected: for instance engine efficiency and exergy destruction are improved by increasing T_1 and K_1 or made worse by increasing I_s , E_x or Q_{leak} .

Table 3: Sensitivity study, optimised centralised power generation (a) Heat engine (b) Heat pump. Term B_{dest} refers to heat engine or heat pump only and excludes indirect terms.

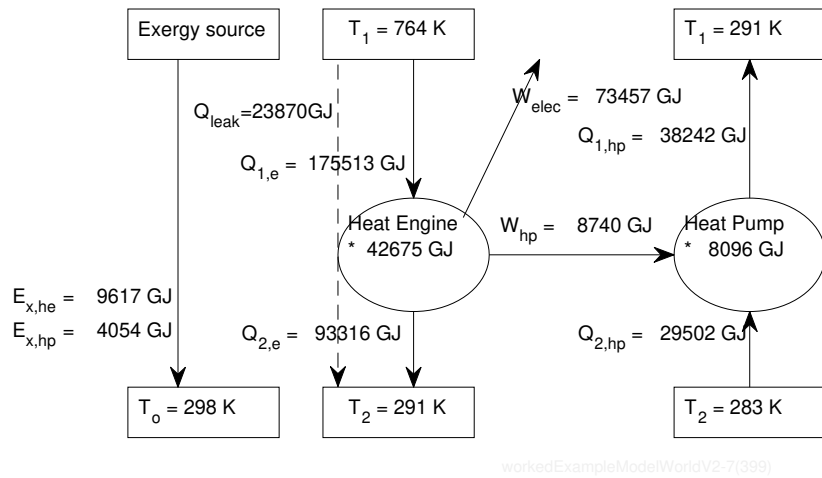
Adjusted	None	I_s	Q_{leak}	T_1	T_1	E_x	K_1
Base val	-	1.1661	$0.13Q_1$	764	764	$0.117 \times W$	$Q_1/(0.5 \times 235K)$
New val	-	1	0	850	1000	$0.234 \times W$	$10 \times Q_1/(0.5 \times 235K)$
T_i, K	666.3	652.5	694.2	736.1	858.1	655.8	726.4
T_j, K	303.8	304.9	299.7	304.6	305.5	305.5	305.4
$\eta_{cyc}, \%$	46.8	53.3	49.7	51.8	58.5	45.7	44.2
$\eta_{plant}, \%$	41.1	46.0	49.7	44.8	49.8	40.2	51.0
$B_{dest}(HE), GJ$	42 675	29 219	20 759	39 337	35 710	45 485	33 635

(a)

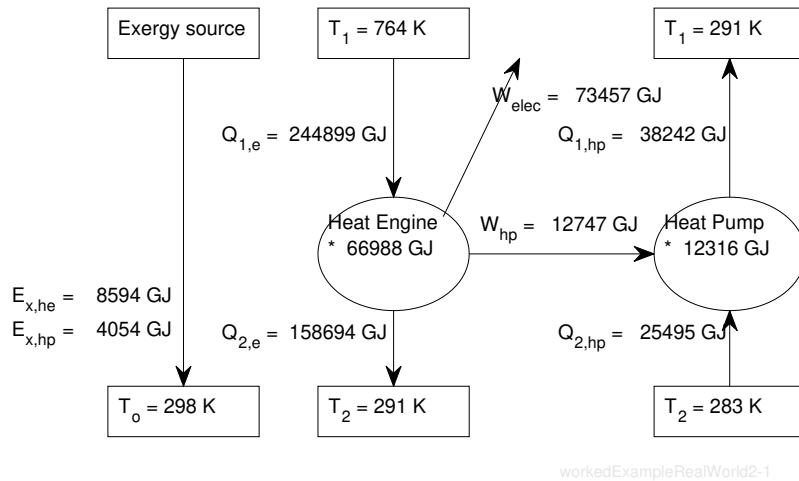
Adjusted	None	I_s	Q_{leak}	T_1	T_1	E_x	K_1
Base val	-	0.9	0.	291	291	$0.106Q_1$	$Q_1/(0.5 \times 15K)$
New val	-	1	$0.1 \times Q_1$	310	330	$0.212Q_1$	$10 \times Q_1/(0.5 \times 15K)$
T_i, K	309.4	308.4	308.7	329.6	350.9	318.6	296.6
T_j, K	265.3	265.3	265.9	265.3	265.3	257.9	265.3
COP_{cyc}	4.38	7.14	4.45	3.63	3.13	3.69	5.13
COP_{plant}	4.38	7.14	4.01	3.63	3.13	3.69	5.13
$B_{dest}(HP), GJ$	8 096	4 532	7 815	9 997	11 767	9 827	6 749

(b)

The associated coefficient of performance of the heat pump was **46% greater than** the present-day value but **8.3 times less than** the Carnot value (Table 2). Given model sensitivities, the closeness of optimum COP to that of a present-day ground source heat pump (about 4) is fortuitous; in Table 3(b) changing $I_s = 0.9$ to $I_s = 1$ yields $COP = 7.14$. On Figure 9, part (a), the two indirect energies were appreciable, equivalent to 23% of exergy destruction attributed to the heat engine and 50% of exergy destruction attributed to the heat pump. Figure 9 part (b) shows results with the present day efficiency and heat pump COP as listed in Table 2. The overall demand for heat was 23% higher than for MLED. Compared to the MLED estimates in part (a) the exergy destruction attributed to the heat engine was 57% greater and that of the heat pump 52% greater than their optimums; [R1:4] the difference in internal temperatures, $T_i > T_i^1$, brings about higher cycle efficiencies in the MLED. The calculated destruction of exergy for the MLED relies on the present day value of E_x . However, the manufacture of an optimised plant would require greater investment and use of energy, for example in the installation of regenerative heating equipment (higher T_i and reduced I_s), larger reheaters (higher T_i), or more expensive superheater materials to permit higher pressures and temperatures (higher T_i) [49] [45]. The additional materials and manufacturing processes could well tend to force higher E_x and thus shift optimum operation towards maximum power conditions. For instance doubling E_x , in isolation, reduced plant efficiency by 0.9% (Table 3(a)).



(a)



(b)

Figure 9: Annual energy flows for centralised power station plus heat pumps: (a) from model of least exergy destruction with engine $I_s = 1.166$, $Q_{leak} = 0.136 \times Q_1 = 23870 \text{ GJ}$ and heat pump $I_s = 0.9$, $Q_{leak} = 0$ (b) from present-day heat engine efficiency and coefficient of performance (Table 2). Rectangles represent thermal reservoirs; the hot reservoir uses the logarithmic mean of the gas inlet and outlet temperatures. Circles represent heat engines and heat pumps; exergy destruction is preceded by an asterisk (*).

Figure 10 shows the annual energy flows and exergy destruction for a district heating scheme. The diagrammatic conventions used in Figure 9 are retained and the hot reservoir temperatures were made identical to allow comparison. Table 4 summarises the efficiencies used in part (b), and the values employed to obtain the theoretical efficiencies used in part (a). In the absence of an optimised heating loop temperature one employed the temperatures for a 3rd generation district heating system. The Brayton cycle efficiency was estimated as 33.1% using the standard air cycle assumptions [50] according to: isentropic efficiencies of 90% for all compressors and expanders; two staged compressors connected via an intercooler,

and a pressure ratio of 2.76 for each compressor. The indirect energy was taken as that for a gas turbine power plant, $E_x = 0.0123 \times W$ and accounting for construction, maintenance and spare parts [40] but omitting such items as such items as exploration, production, storage, processing and transmission, given that gas was freely available from landfill. Infinite heat transmittance to the cold reservoir, $K_2 \rightarrow \infty$, was assumed and transmittance K_1 was estimated from Equation 9 with $g = 0.5$ and $T_1 - T_i^1 = 55K$. [51]

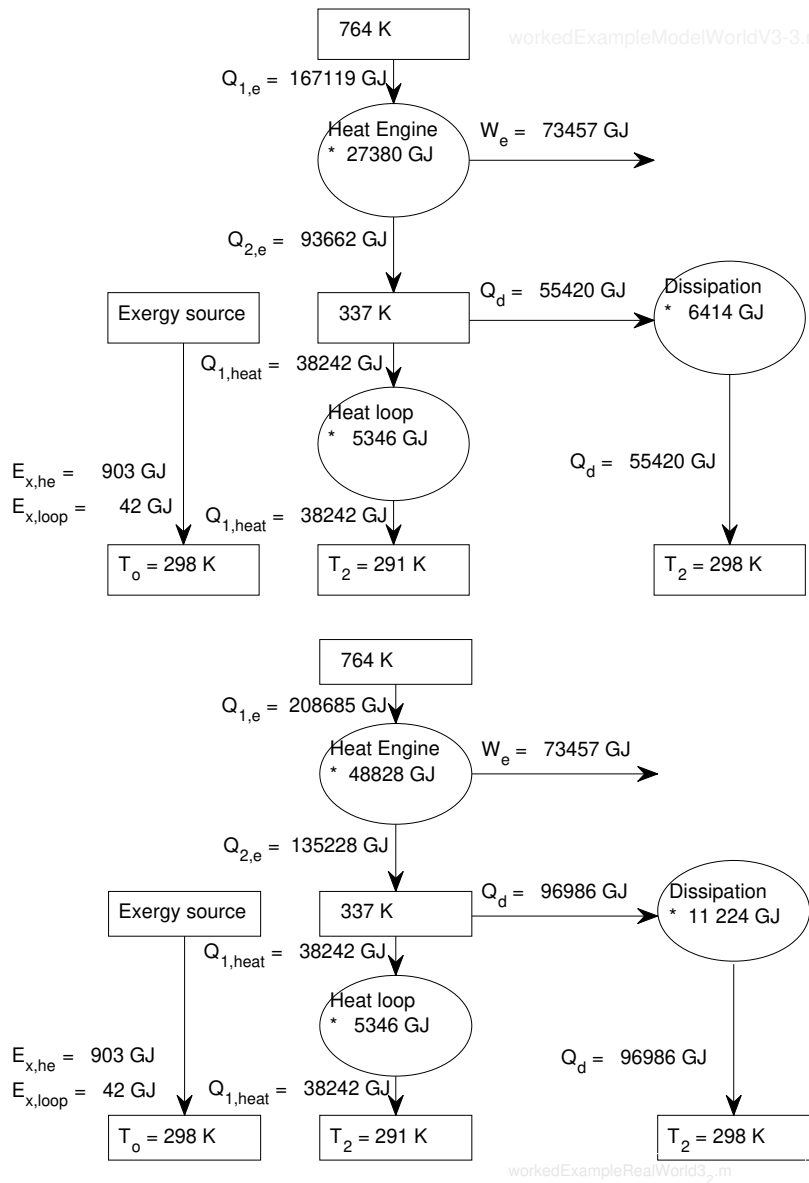
Table 4: Efficiencies for a local **gas turbine** and district heating.

Heat Engine			District Heating Loop		
Item	Value	Notes	Item	Value	Notes
<u>Present-day values</u>			<u>Present-day values</u>		
Efficiency	33.1%				
<u>Estimates for optimisation</u>			<u>Estimates for optimisation</u>		
E_x/W	0.0123	[40]	E_x/Q	1.1×10^{-3}	Table 1
I_s	1.166		T_2	283K	
T_1	764K		T_1	337K	
T_2	337K				
T_i^1 [51]	$T_1 - 55K$	Provisional, to get K_1			
T_j	$T_j \rightarrow T_2$	$K_2 \rightarrow \infty$			
<u>Efficiencies</u>					
Present day	33.1%				
MLED	44.0%				
Carnot	55.9%				
Maximum Power [5]	33.6%				

The analysis from the model of **least exergy production** is presented on Part (a) of Figure 10, as well as Table 4. Performance is superior to that of the centralised generation of electricity (Figure 9). The total **annual destruction of exergy** is somewhat less: **50 771GJ** in Figure 9(a) versus **39 140GJ** in Figure 10(a). There is also a **reduction of 16% in demand for heat** but an appreciable reduction in **annual indirect energy** from **13 671GJ** to **945GJ**.

Figure 10 (b) relates to the present-day estimates. About **25%** more heat is needed than in part (a) and the annual **destruction of exergy** is increased **by 67% to 65 398GJ**. This is still less than the **79 304GJ destruction** for centralised generation of electricity, shown in Figure 10(b).

Some overarching comments follow. **For assumed parameters, in terms of both present-day and MLED estimates, localised generation of electricity with district heating appears slightly superior to the centralised generation of electricity. For instance the demand for heat ($Q_1 + Q_{leak}$) is reduced by 16.2% according to the MLED and by 14.8% according to the present-day estimates. Carrying out the worked examples causes certain themes to emerge. The very different amounts of indirect energy associated with different plant has some influence on evaluation outcomes. (The gas turbine required substantially less indirect energy than the coal plant.) Although is intended as a first estimate. the MLED is sensitive to uncertainties in its input parameters (E_x, I_s, K_1, K_2) and such sensitivity, coupled with the lack of modelling structure, is important. The apparent differences in heat supply Q_1 , and B_{dest} , between centralised and local generation (roughly $B_{dest} = 51TJ$ versus $39TJ$) merely support a far more detailed analysis; they do not in themselves justify adoption of a local scheme. Similar reasoning applies when one considers the proposition that centralised plant should be upgraded to achieve greater efficiency.**



(a)

(b)

Figure 10: Annual energy flows for a District Heating scheme, fueled from landfill gas. (a) Idealised process. Heat leak of $0.136 \times Q_1$ not shown (b) heat engine efficiency of 33.1%. See Figure ?? for symbols and Table xx 4 for operating parameters.

Nonetheless, the differences between the MLED and present-day estimates can indicate broadly opportunities to minimise irreversibilities by reducing the driving temperature differences. For instance, in some commercial demonstration Advanced-Ultra Super Critical power plant cycle efficiencies above 50% are possible because, in part, new tube and pipe super alloys enable temperatures of superheated steam (T_i in the MLED) to be increased from 550°C to in the region of 760°C [49] [45]. [R1:5.5]

In the comparison of two energy schemes the **exergetic losses** in combustion, to produce gases at 1300 K, was ignored but assumed to be equivalent for the two scenarios. More importantly, the global warming potential of methane - potentially leaked from the landfill site - was outside the scope of this article but should be considered by environmental consultants.

For the worked example the source of heat cooled appreciably, from 1300K to 400K. The logarithmic mean was taken as equivalent to the single temperature of a hot reservoir. This substitution would yield zero net entropy production for a reversible heat engine.

Maximum power and Carnot efficiencies offer simple, rapid calculations intended to provide an upper bound on efficiency, in advance of either rapidly discounting a proposed scheme or moving to a more detailed calculation. The MLED necessitates **estimates for I_s and thermal transmittance** but otherwise by far the most taxing aspect lies in researching the indirect energy. It is conceivable that new, high temperature materials, larger heat exchanger surfaces, and more complex plant will improve efficiency but at the cost of higher indirect energy use, thereby making the methods presented here more relevant. Indirect energy use would clearly be higher for longer district heating networks. For instance a branched network installed in 1988 in Ishoej, Demmark extends for 8.7 km [52]. Moreover, the indirect energy of district heating might be more than in Table 1 because we had no access to databases allowing for contributions such as manual labour and the transportation of turbines and piping.

6. Conclusions

Internally reversible engines have been tackled with a functional model of least **exergy destruction (MLED)**, with allowances for thermal resistance between the engine and **its reservoirs, heat leaks and internal irreversibility**. **The model make a further** allowance for the indirect use of energy. The MLED is intended for the rapid screening of numerous candidate schemes for power generation, as a preliminary to more detailed and costly structural analysis. **For endoreversible engines ($I_s = 1$) with no heat leak, and with large use of indirect energy, the optimum hot engine fluid temperature (T_i) and cycle efficiency tended towards the maximum power limit.** With zero use of indirect energy the Carnot limit was achieved.

With regards to heat pumps, a **conditional** optimum coefficient of performance is evident **The minimum point is far less distinct than that for heat engines.**

A worked example is provided , **to demonstrate the potential for methods such as MLED to be employed prior to the first of many stage-gate decisions.** The local generation of power required less heat and **destroyed less exergy** with both present-day and MLED estimates of efficiency; this would justify further investigation with more detailed, structural models. **However, the functional nature of the model and uncertainties in model parameters restrict its practical use to the preliminary screening of design options.**

7. Data Access

The MATLAB code developed for this paper is available at https://data-bris.acrc.bris.ac.uk/projects/Thermal_Coatings.

8. References

References

- [1] G. F. Rogers, Y. R. Mayhew, *Engineering Thermodynamics Work & Heat Transfer*, Longman Group Limited, 1980 (1980).
- [2] S. Carnot, *Réflexions sur la puissance motrice du feu et sur les machines propres à développer cette puissance*, in: *Annales scientifiques de l'École Normale Supérieure*, Vol. 1, 1872, pp. 393–457 (1872).
- [3] Y. Haseli, *Entropy Analysis in Thermal Engineering Systems*, Academic Press, 2019 (2019).
- [4] J. H. Cotterill, *The Steam Engine Considered as a Thermodynamic Machine: A Treatise on the Thermodynamic Efficiency of Steam Engines*, E. and FN Spon, 1896 (1896).
- [5] I. Novikov, The efficiency of atomic power stations (a review), *Journal of Nuclear Energy* (1954) 7 (1-2) (1958) 125–128 (1958).
- [6] F. Curzon, B. Ahlborn, Efficiency of a Carnot engine at maximum power output, *American Journal of Physics* 43 (1) (1975) 22–24 (1975).
- [7] E. P. Gyftopoulos, Fundamentals of analyses of processes, *Energy Conversion and Management* 38 (15-17) (1997) 1525–1533 (1997).
- [8] J. Chen, Z. Yan, G. Lin, B. Andresen, On the Curzon–Ahlborn efficiency and its connection with the efficiencies of real heat engines, *Energy Conversion and Management* 42 (2) (2001) 173–181 (2001).
- [9] K. H. Hoffmann, An introduction to endoreversible thermodynamics, *Atti dell Accademia Peloritana dei Pericolanti-Classe di Scienze Fisiche, Matematiche e Naturali* 86 (2008) 1–6 (2008).
- [10] C. Blanchard, Coefficient of performance for finite speed heat pump, *Journal of Applied Physics* 51 (5) (1980) 2471–2472 (1980).
- [11] F. Sun, W. Chen, L. Chen, C. Wu, Optimal performance of an endoreversible Carnot heat pump, *Energy Conversion and Management* 38 (14) (1997) 1439–1443 (1997).
- [12] W. Muschik, K. H. Hoffmann, Endoreversible thermodynamics: A tool for simulating and comparing processes of discrete systems, *Journal of Non-Equilibrium Thermodynamics* 31 (3) (2006) 293–317 (2006).
- [13] L. Onsager, Reciprocal relations in irreversible processes. i., *Physical review* 37 (4) (1931) 405 (1931).
- [14] R. H. Winterton, Early study of heat transfer: Newton and Fourier, *Heat Transfer Engineering* 22 (5) (2001) 3–11 (2001).
- [15] A. De Vos, Endoreversible thermoeconomics, *Energy conversion and management* 36 (1) (1995) 1–5 (1995).
- [16] A. De Vos, Endoreversible economics, *Energy conversion and management* 38 (4) (1997) 311–317 (1997).
- [17] A. Bejan, Power and refrigeration plants for minimum heat exchange inventory., *Journal of Energy Resources Technology. Transactions of the ASME* 115 (2) (1993) 148–150 (1993).
- [18] O. Ibrahim, S. Klein, J. Mitchell, Optimum heat power cycles for specified boundary conditions, *Journal of Engineering for Gas Turbines and Power* 113 (4) (1991) 514–521 (1991).
- [19] P. Salamon, A. Nitzan, B. Andresen, R. S. Berry, Minimum entropy production and the optimization of heat engines, *Physical Review A* 21 (6) (1980) 2115 (1980).
- [20] F. Angulo-Brown, An ecological optimization criterion for finite-time heat engines, *Journal of Applied Physics* 69 (11) (1991) 7465–7469 (1991).

- [21] L. A. Arias-Hernandez, F. Angulo-Brown, A general property of endoreversible thermal engines, *Journal of applied physics* 81 (7) (1997) 2973–2979 (1997).
- [22] C.-Y. Cheng, et al., Ecological optimization of an irreversible brayton heat engine, *Journal of Physics D: Applied Physics* 32 (3) (1999) 350 (1999).
- [23] S. Tyagi, S. Kaushik, R. Salhotra, Ecological optimization and performance study of irreversible stirling and ericsson heat engines, *Journal of Physics D: Applied Physics* 35 (20) (2002) 2668 (2002).
- [24] M. A. Barranco-Jimenez, F. Angulo-Brown, Thermoeconomic optimisation of novikov power plant model under maximum ecological conditions, *Journal of the Energy Institute* 80 (2) (2007) 96–104 (2007).
- [25] Z. Yan, Comment on “a general property of endoreversible thermal engines”[*j. appl. phys.* 81, 2973 (1997)], *Journal of Applied Physics* 89 (2) (2001) 1518–1519 (2001).
- [26] F. Angulo-Brown, L. A. Arias-Hernandez, Reply to “comment on ‘a general property of endoreversible thermal engines’”[*j. appl. phys.* 89, 1518 (2001)], *Journal of Applied Physics* 89 (2) (2001) 1520–1521 (2001).
- [27] D. Agrawal, V. Menon, Finite-time carnot refrigerators with wall gain and product loads, *Journal of applied physics* 74 (4) (1993) 2153–2158 (1993).
- [28] S. Velasco, J. Roco, A. Medina, A. Calvo Hernandez, Irreversible refrigerators under per-unit-time coefficient of performance optimization, *Applied physics letters* 71 (8) (1997) 1130–1132 (1997).
- [29] A. Bejan, Entropy generation minimization: The new thermodynamics of finite-size devices and finite-time processes, *Journal of Applied Physics* 79 (3) (1996) 1191–1218 (1996).
- [30] J. Chen, The maximum power output and maximum efficiency of an irreversible carnot heat engine, *Journal of Physics D: Applied Physics* 27 (6) (1994) 1144 (1994).
- [31] A. Bejan, *Advanced engineering thermodynamics*, John Wiley & Sons, 2016 (2016).
- [32] T. J. Kotas, *The exergy method of thermal plant analysis*, Elsevier, 2013 (2013).
- [33] B. Sayin Kul, A. Kahraman, Energy and exergy analyses of a diesel engine fuelled with biodiesel-diesel blends containing 5% bioethanol, *Entropy* 18 (11) (2016) 387 (2016).
- [34] R. Frischknecht, N. Jungbluth, H.-J. Althaus, G. Doka, R. Dones, T. Heck, S. Hellweg, R. Hischier, T. Nemecek, G. Rebitzer, et al., The ecoinvent database: Overview and methodological framework (7 pp), *The international journal of life cycle assessment* 10 (1) (2005) 3–9 (2005).
- [35] U. R. Fritsche, K. Schmidt, *Global emission model of integrated systems (gemis)*, Institute for Applied Ecology (2008).
- [36] E. Terehovics, I. Veidenbergs, D. Blumberga, Exergy analysis for district heating network, *Energy Procedia* 113 (2017) 189–193 (2017).
- [37] W. P. Brinckerhoff, *Avonmouth and severnside heat network study - heat mapping report* (2015).
URL http://www.southglos.gov.uk/documents/20151201_Avonmouth_Severnside_Heat_Mapping_Report_RevB.pdf
- [38] X. Wu, X.-H. Xia, G. Chen, X. Wu, B. Chen, Embodied energy analysis for coal-based power generation system—highlighting the role of indirect energy cost, *Applied energy* 184 (2016) 936–950 (2016).
- [39] B. Greening, A. Azapagic, Domestic heat pumps: Life cycle environmental impacts and potential implications for the UK, *Energy* 39 (1) (2012) 205–217 (2012).
- [40] P. Meier, K. GL, *Life-cycle energy cost and greenhouse gasemissions for gas turbine power* (2000).
URL <https://www.seventhwave.org/sites/default/files/202-1.pdf>
- [41] O. Martin-Du Pan, P. Woods, R. Hanson-Graville, Optimising pipe sizing and operating temperatures for district heating networks to minimise operational energy consumption, *Building Services Engineering Research and Technology* 40 (2) (2019) 237–255 (2019).
- [42] Greater London Authority, *District heating manual for london* (2013).
URL https://www.cibse.org/getmedia/843f2dbd-55eb-4c6c-b219-88fe9eb83949/DH_Manual_for_London_February_

2013_v1-0.pdf.aspx

- [43] T. Chen, J. Burnett, C. Chau, Analysis of embodied energy use in the residential building of Hong Kong, *Energy* 26 (4) (2001) 323–340 (2001).
- [44] L. P. Devi, S. Palaniappan, A study on energy use for excavation and transport of soil during building construction, *Journal of Cleaner Production* 164 (2017) 543–556 (2017).
- [45] C. Wales, M. Tierney, M. Pavier, P. E. Flewitt, Reducing steam transport pipe temperatures in power plants (in press), *Energy* (2019).
- [46] G. F. Hundy, *Refrigeration, air conditioning and heat pumps*, Butterworth-Heinemann, 2016 (2016).
- [47] E. Silberstein, *Heat pump basics* (2014).
URL <https://heatinghelp.com/systems-help-center/heat-pump-basics/>
- [48] Mitsubishi, Product information, CAHV-P500YA-HPB ecodan air source heat pump (2015).
URL http://library.mitsubishielectric.co.uk/pdf/book/CAHV-P500YHA-HPB_PI_Sheet#page-1-2
- [49] P. S. Weitzel, Component test facility (COMTEST) phase 1 engineering for 760C (1400F) advanced ultra-supercritical (A-USC) steam generator development, in: ASME 2015 Power Conference collocated with the ASME 2015 9th International Conference on Energy Sustainability, the ASME 2015 13th International Conference on Fuel Cell Science, Engineering and Technology, and the ASME 2015 Nuclear Forum, American Society of Mechanical Engineers, 2015, pp. V001T10A003–V001T10A003 (2015).
- [50] Y. A. Cengel, M. A. Boles, *Thermodynamics: An Engineering Approach - Seventh Edition*, McGraw-Hill Companies, 2011 (2011).
- [51] P. Wolfe, H. F. May, Design and experience with regenerators for industrial gas turbines, in: ASME 1969 Gas Turbine Conference and Products Show, American Society of Mechanical Engineers, 1969, pp. V001T01A075–V001T01A075 (1969).
- [52] H. V. Larsen, B. Bøhm, M. Wigbels, A comparison of aggregated models for simulation and operational optimisation of district heating networks, *Energy Conversion and Management* 45 (7-8) (2004) 1119–1139 (2004).
- [53] N. A. Cumpsty, *Compressor aerodynamics*, no. BOOK, Longman Scientific & Technical, 1989 (1989).
- [54] J. Marion, O. Drenik, C. Frappart, F. Kluger, M. Sell, A. Skea, R. Vanstonee, P. Walker, Advanced ultra-supercritical steam power plants, in: Proc IEA Clean Coal Centre Workshop: Advanced Ultrasupercritical Coal-fired Power Plants, 2012, pp. 4–2 (2012).

Appendix 1 Estimates of the Irreversibility Factor

No published values were found for the cycle irreversibility parameter, I_s . Let us consider an initially reversible cycle operating such that heat is added to working fluid at constant temperature and rejected from working fluid at constant temperature. (An example is the hypothetical reversible vapour cycle in [1].) It is required to find the increased heat rejection, $|Q_2|$, owing to internal irreversibilities. The irreversibility factor is then

$$I_s = \frac{|\Delta S_2|}{|\Delta S_1|} = \frac{|Q_2/T_2|}{Q_1/T_1}$$

Then let the performance be degraded by non-ideal compressor and turbine isentropic efficiencies, typically $\eta_{t,is} \approx \eta_{c,is} \approx 90\%$ [53] [54] such that Q_1 is unaffected and $|Q_2|$ is increased. The First Law yields reversible

and irreversible Q_2 .

$$Q_2(rev) = -Q_1 - W_{t,is} - W_{c,is}$$

$$Q_2(irrev) = -Q_1 - W_{t,is}\eta_{t,is} - \frac{W_{c,is}}{\eta_{c,is}}$$

For the resersible case $I_s = 1$ fand $Q_1/T_1 = |Q_2(rev)|/T_2$.

$$\frac{Q_2(irrev)}{T_2} = \frac{Q_2(rev)}{T_2} + \frac{W_{t,is}(1 - \eta_{t,is}) + W_{c,is}(1 - 1/\eta_{c,is})}{T_2}$$

$$= \frac{Q_2(rev)}{T_2} + \frac{W_{rev}(1 - \eta_{t,is} - R_{bw}\eta_{t,is}\eta_{c,is} + R_{bw}\eta_{c,is})}{T_2(1 + R_{bw}\eta_{t,is}\eta_{c,is})}$$

Where $R_{bw,rev}$ is the back work ratio of irreversible compressor work to irreversible turbine power. Now employ the Carnot efficiency to obtain reversible cycle work.

$$\frac{Q_2(irrev)}{T_2} = \frac{Q_2(rev)}{T_2} + \frac{Q_1(1 - T_2/T_1)}{T_2} \frac{(1 - \eta_{t,is} - R_{bw}\eta_{t,is}\eta_{c,is} + R_{bw}\eta_{t,is})}{(R_{bw}\eta_{t,is}\eta_{c,is})}$$

Multiply the above by T_1/Q_1 to get the adjustment to I_s

$$I_s = 1 + \frac{(T_1 - T_2)}{T_2} \frac{(1 - \eta_{t,is} - R_{bw}\eta_{t,is}\eta_{c,is} + R_{bw}\eta_{t,is})}{(1 + R_{bw}\eta_{t,is}\eta_{c,is})}$$

Typical values are 90% for compressor and turbine efficiencies [53] and 30% for the back work ratio, so that $I_s = 1.17$.